Journal of Alloys and Compounds 520 (2012) 98–104

Contents lists available at SciVerse ScienceDirect

Journal of Alloys and Compounds

journal homepage: www.elsevier.com/locate/jallcom

Preferred hydride growth orientations on oxide-coated gadolinium surfaces

G.M. Benamar[a,b], D. Schweke[a,*], G. Kimmel[b], M.H. Mintz[a,b]

[a] Nuclear Research Centre Negev, P.O. Box 9001, Beer-Sheva 84190, Israel
[b] Deparment of Nuclear Engineering, Ben-Gurion University, P.O. Box 653, Beer-Sheva 84105, Israel

ARTICLE INFO

Article history:
Received 23 December 2011
Accepted 26 December 2011
Available online 2 January 2012

Keywords:
Gadolinium hydride
Growth orientations
X-ray diffraction

ABSTRACT

The initial development of hydrides on polycrystalline gadolinium (Gd), as on some other hydride forming metals, is characterized by two sequential steps. The first step involves the rapid formation of a dense pattern of small hydride spots (referred to as the "small family" of hydrides) below the native oxidation layer. The second stage takes place when some of the "small family" nucleants (referred to as "growth centers", GCs) break the oxide layer, leading to their rapid growth and finally to the massive hydriding of the sample.

In the present study, the texture of the two hydride families was studied, by combining X-ray diffraction (XRD) analysis with a microscopic analysis of the hydride, using scanning electron microscopy (SEM) and atomic force microscopy (AFM). It has been observed that for the "small family", a preferred growth of the $(1\,0\,0)_h$ plane of the cubic GdH_2 takes place, whereas for the GCs, a change to the $(1\,1\,1)_h$ plane of the cubic hydride dominates. These preferred growth orientations were analyzed by their structure relation with the $(0\,0\,.1)_m$ basal plane of the Gd metal.

It has been concluded that the above texture change is due to the surface normal compressive stress component exerted by the oxidation overlayer on the developing hydride, preventing the $(0\,0\,.1)_m||(1\,1\,1)_h$ growth orientation. This stress is relieved upon the rupture of that overlayer and the development of the GCs, leading to the energetically favorable mode of growth.

1. Introduction

When a hydride-forming metal is exposed to hydrogen under proper pressure–temperature conditions, development of hydride precipitates starts at the near-surface region. The incipient stages of this process were defined in previous publications [1,2] and include hydrogen chemisorption on the oxide surface, permeation of the hydrogen atoms in the oxide and their diffusion towards the oxide–metal interface and build-up of the hydrogen concentration in the metal, nearby the interface. The formation of hydride nuclei was often characterized by two sequential steps [1–4] especially for binary M–H systems under "real life" conditions (i.e., polycrystalline metals coated by some thin oxidation overlayers).

During the first stage, a dense pattern of tiny (sub-micron) hydride spots are formed beneath the oxidation overlayer that coats the metallic surface [1–4]. The appearance of these spots is very rapid, within a few seconds after the exposure to hydrogen. The spots grow with an exponentially decelerating rate, reach their final size (in the range of about 0.5–1 μm), and practically cease a noticeable further development [4]. Following the above stage, after a certain "induction time" (which depends on the pressure–temperature conditions) certain hydride spots start further development. Those spots, referred to as growth centers (GCs), grow rapidly at a roughly constant rate, thus spreading over the surface and finally leading to the massive hydriding of the sample. The development of those GCs also depends on the experimental pressure–temperature conditions and this dependence has been accounted for by a proper kinetic model [2]. It has been proposed [1–3] that the transition between the initial hydride spots and the formation of GCs involves the rupture of the oxide layer, thus relieving the stress field exerted on the hydride spot and enabling its further development [5].

The characteristics of the hydride nuclei (location, density and growth kinetics) depend both on the microstructure of the metal from which they develop and on the coating oxidation overlayer. The former contribution has been evidenced by measurements performed on the U–H system in which the uranium hydride nuclei were found to form on grain boundaries or twin boundaries of the metal [6,7] or at inclusion sites [8]. In addition, the contribution of the metal texture on hydride nucleation has been pointed out regarding the different number densities of hydride nuclei observed on different metal grains of the Gd [4]. The underlying

* Corresponding author.
E-mail address: daniela.schweke@gmail.com (D. Schweke).

0925-8388/$ – see front matter © 2012 Elsevier B.V. All rights reserved.
doi:10.1016/j.jallcom.2011.12.127

metal microstructure therefore seems to have an influence on the location of the initial hydride nucleation sites and on their densities. On the other hand, the surface oxidation overlayer may affect the nucleation and growth characteristics of the hydride through several factors:

(i) Chemisorption related effects: Some functional groups (such as hydroxyls) present on the topmost surface layer of the oxide may impede the dissociative chemisorption of the gaseous H_2 molecules, thereby affecting the ingress flux of H atoms [9,16,17].
(ii) Diffusion related effects: The thickness, composition, and microstructure of the oxidation overlayer may affect the diffusion rate of H atoms across that layer, thereby affecting the build-up of dissolved H concentration at the oxide–metal interface region, which leads to hydride nucleation (e.g. ref. [10]).
(iii) Mechanical related effects: The compression of an intact oxidation overlayer on the expanding hydride nuclei (developing beneath that layer), may affect the growth rates of these nuclei [5] and their geometry [11].

Yet, another mechanical related effect, that so far has not been pointed out, is the texture of the growing hydride nuclei. It is well known that some growth planes of hydrides are preferred for certain habit planes of the parent metal (e.g. the (1 1 1) plane of the δ-ZrH_x that precipitates on the (0 0 .1) plane of the Zr [12–15]). Such orientation relations which usually originate from minimization of misfit strain energies at the interfaces between the original metal and the formed hydride product may be altered by an additional stress field parameter exerted by the oxidation overlayer. The transition between a mechanically stressed process that characterizes the "small family" development, and a "stress-free" process that controls the GCs development [5], may in turn not only affect the growth rates of the two families [5] but may also be manifested in some texture changes displayed by these families.

In the present study, X-ray diffraction (XRD) measurements were performed on polycrystalline Gd surfaces, with different quantities of the two precipitated hydride families. The amount of the GCs relative to the small spots family was monitored through the reaction temperature (in the range of 295–623 K), keeping the pressure–time conditions constant (6 mbar H_2, 480 s exposure). Under these experimental conditions, appearance of the GCs started at temperatures above ~473 K, concurrent with differences in the texture patterns of the hydride. In the following discussion these observations are interpreted in terms of preferred orientation relations between some planes of the formed hydride (cubic cF12–CaF_2 type–GdH_2) and the hexagonal basal plane of the parent metal (hP2 Mg type–Gd) and by the stress related characteristics of these growth orientations.

2. Experimental

Polycrystalline Gd samples, of grain size in the range of 50–100 μm, cut from an as-casted rod were polished down to 1 μm roughness. Hydrogen exposure experiments of the Gd samples were performed in a so-called hot stage microscope (HSM), enabling in-situ monitoring of the reaction between the heated sample and hydrogen using a small magnification microscope. This system was used in previous studies and described in detail in reference [4]. After introduced into the high-vacuum chamber (base pressure of about 10^{-6} mbar), the samples were activated under vacuum for 1 h at 473 K [16,17] and finally cooled down or heated to the pre-determined exposure temperature. The effect of the heat activation process on the sample's reactivity has been recently studied [17] and attributed to desorption of surface hydroxyl species present on top of the native oxidation layer. Auger depth profiling performed on the samples before and after the pre-heating process indicated that the thickness of the oxidation layer slightly increased (from 3–4 nm to 8–10 nm) following the heat pretreatment, due to oxidation by residual vapor present in the reactor.

After the activation stage, ultra-pure hydrogen produced by heating a uranium hydride bed was admitted to the chamber at the given reaction temperature and evacuated after reaching a pre-determined exposure time. In the present study, experiments were performed in the temperature range of 295–623 K. The hydrogen pressure and exposure time were chosen so as to focus on the initial development of the hydride. Therefore, a low hydrogen pressure of 6 mbar and rather short exposure time of 8 min were applied.

The characteristics of the hydride nuclei thus formed on the sample surface were analyzed using optical microscopy, scanning electron microscopy (SEM) and atomic force microscopy (AFM). The pictures obtained using the latter method were used to determine the dimensions (width and height) of each of the hydride spots observed and to evaluate the average area covered by the hydride phase. Histograms representing the distribution of the hydride nuclei height and diameter were thus built from each of the experiment. In addition X-ray diffraction measurements were performed on these samples after these exposures. The X-ray diffraction system was a θ–2θ Philips PW3020 Bragg–Brentano powder diffractometer, powered by PW1730 generator. The diffraction data was collected by step scanning between 10° and 70° 2θ with a step equal to 0.02° and a count time of 10 s/step. The experimental conditions were: diffracted-beam graphite (0 0 .2) monochromator, Cu Kα radiation, and 45 kV and 40 mA, divergence and anti-scattering slits 1°, receiving slit 0.2 mm. For data processing, SRM 1976 (corundum) was used as line position standard. Rietveld's method [18–20] was applied for data processing using the public domain program powder-cell [21]. Integrated intensities were retrieved from the diffractograms by using line profile fitting (LPF) from PC-APD Philips software.

3. Results

3.1. Characteristics of the hydride nuclei as a function of temperature

In the whole temperature range studied, sub-micron hydride spots were observed on the sample surface. As reported previously [4], the density of these spots varied for different grains. However, the average surface coverages were quite reproducible, and ranged between 5 and 8% for the whole temperature range. The dimensions of the hydride spots (mean height and area) as well as their average surface coverage as deduced from the AFM analysis are listed in Table 1. In a previous work [4], these small hydride spots were found to appear within a few seconds of exposure to hydrogen and to rapidly reach their final size.

As can be seen from Table 1, the average lateral size of the spots as well as the spread in their lateral size distribution increased with increasing temperature. At temperatures above about 498 K, hydride spots of rather high diameter (1 μm and more) could be discerned. This can be seen in the histograms representing the distribution of the hydride nuclei diameter at those temperatures (Fig. 1) in which a "tail" extending to high diameter values appears. This is also evident in the data listed in Table 1, displaying higher values of the nuclei mean diameters and of the diameter's standard deviations at temperatures higher than ~498 K. In addition, in those conditions, hydride "GCs" of ~10 μm diameter and more were observed in optical and scanning electron microscopic pictures, as shown in Fig. 2. The latter strongly differ from the hydrides belonging to the "small family": they appeared at very low densities and were not distributed uniformly on the surface. In addition, they apparently caused breaking of the oxide layer whereas the sub-micron hydride nuclei grew under the intact oxidation layer coating the metal.

3.2. X-ray diffraction results

The diffractograms recorded form the polycrystalline Gd samples after exposure to hydrogen at several temperatures are exhibited in Fig. 3. A (2 0 0) preferred orientation of the hydride nuclei formed upon Gd can clearly be seen at the lower temperature range. We attempted to perform a quantitative analysis of the hydride orientations versus temperature. The Rietveld method is a strong tool for quantitative and qualitative phase analysis of crystalline powders. However, in the present system, the Gd substrate is a bulk solid sample whereas the hydride and oxide are thin transparent layers. Therefore, only the relative amounts of the

Table 1
Summary of the data concerning the "small family" hydrides deduced from analysis of the AFM pictures.

T [K]	Average area covered by hydride spots (% of surface area)	Nuclei mean height (μm)	Standard deviation	Nuclei mean diameter (μm)	Standard deviation
297	7	0.08	0.04	0.5	0.2
323	7	0.10	0.07	0.6	0.3
338	8	0.09	0.05	0.8	0.4
373	8	0.10	0.07	0.7	0.3
383	8	0.10	0.05	0.7	0.4
413	7	0.08	0.06	0.7	0.5
473	6	0.10	0.05	0.7	0.3
498	8	0.10	0.05	1.3	0.7
523	7	0.10	0.04	1.3	1.1

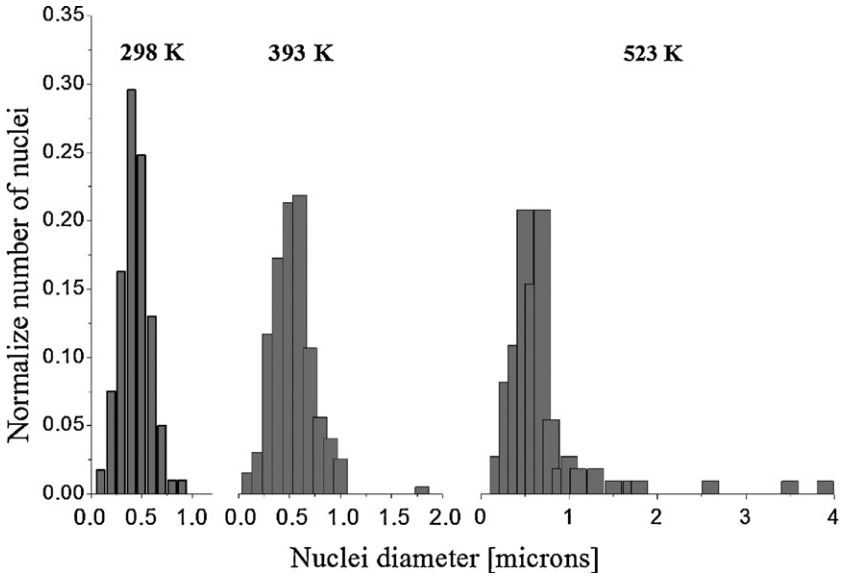

Fig. 1. Histograms representing the distribution of the hydride nuclei diameters obtained from the AFM measurements at different temperatures (298 K, 393 K and 523 K).

polycrystalline hydride and oxide phases could be evaluated. It was found that for hydriding performed up to 473 K, no crystalline oxide was observed and the hydride had a strong preferred orientation in which only the 2 0 0 line appeared in the diffractogram (Fig. 3). Above about 498 K, a randomly oriented crystalline oxide appeared and the 1 1 1 reflection of GdH_2 was detected. When the hydrogenation was performed at higher temperatures, the dominant growth direction of the hydride normal to the surface turned from ⟨1 0 0⟩ to ⟨1 1 1⟩ (Fig. 3). The data deduced from the Rietveld and LPF analyses is summarized in Table 2. As can be seen, the normalized relative ratio of the 1 1 1/2 0 0 hydride intensities is negligible below 473 K and starts to increase for temperatures above ~498 K.

The GCs coverage was estimated at the different temperatures from the metallographic pictures. The estimated coverage thus obtained also appears in Table 2. A good correlation was obtained between the hydride orientation intensity ratio 1 1 1/2 0 0 deduced

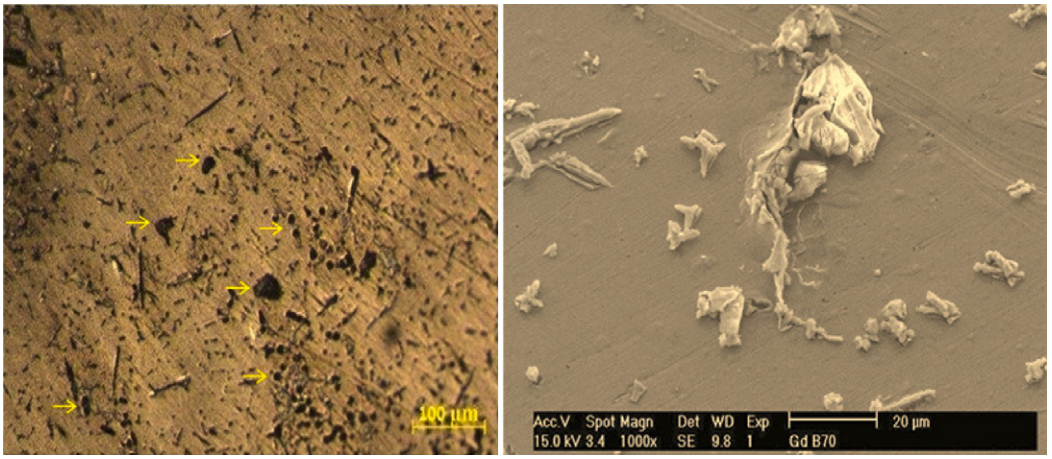

Fig. 2. Metallographic (left) and SEM (right) pictures showing the bigger hydride precipitates above which the oxide layer has been ruptured. These are the initial development centers of the so-called "growth centers" (GCs). The main GCs on the metallographic picture are indicated by arrows.

Table 2
Intensities of selected reflections from GdH_2 and Gd_2O_3 in the X-ray diffractograms at the different temperatures studied.

T [K]	Intensities of all GdH_2 reflections		Intensities of mainGd_2O_3 reflections		Ratio of intensities between 1 1 1 and 2 0 0 reflections for GdH_2	Estimated coverage of Growth Centers on samples' surfaces [%]
	2 0 0	1 1 1	2 2 2	4 0 0		
297	17	0		–	0	0
323	18	0		–	0	0
338	30	0		–	0	0
373	18	0		–	0	0
383	36	0		–	0	0
413	16	0		–	0	0
473	8	0		–	0	2
498	29	118	0	21	4	3.5
523	14	73	106	25	5	4
573	4	38	79	33	9.5	7

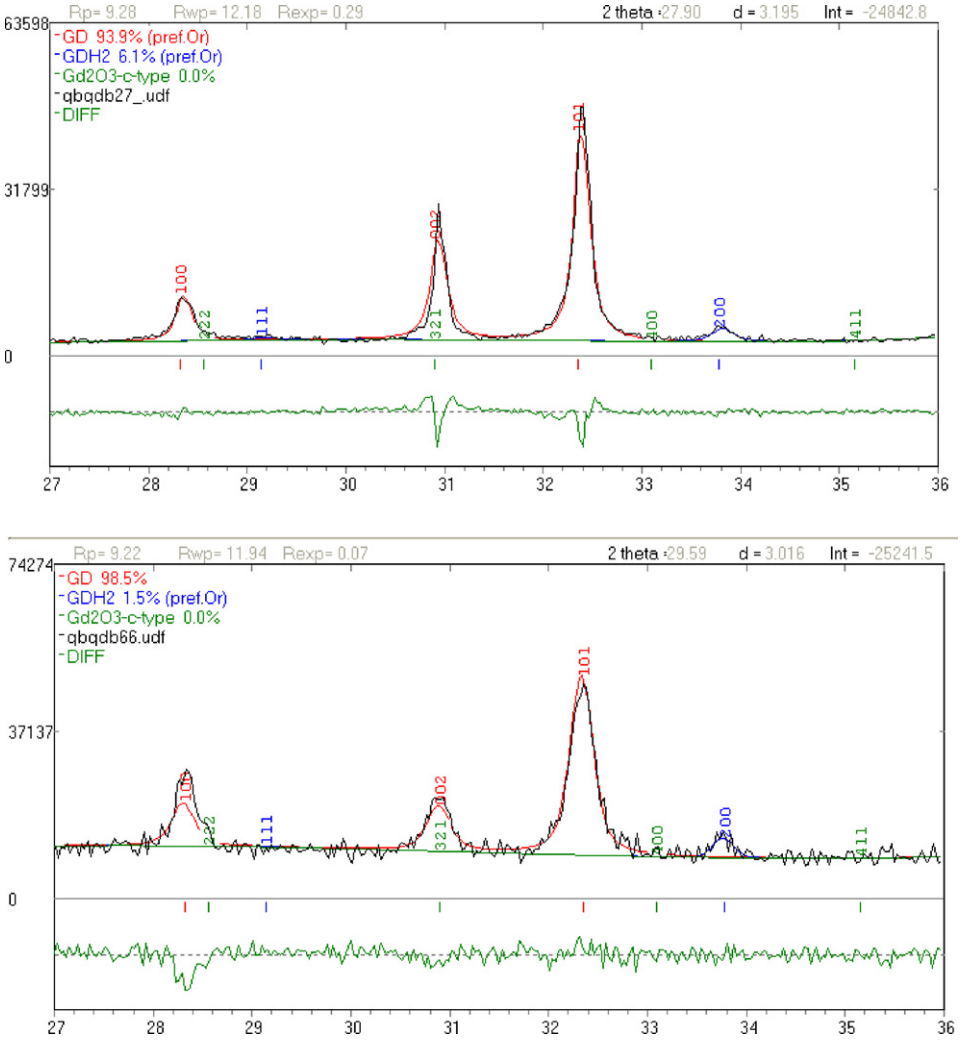

Fig. 3. Rietveld diagrams of Gd samples after exposure to H_2 at 6 mbar for 8 min at the following temperatures: 373 K, 473 K, 498 K, and 573 K (up to bottom). The reflection intensity is given in arbitrary units versus 2θ.

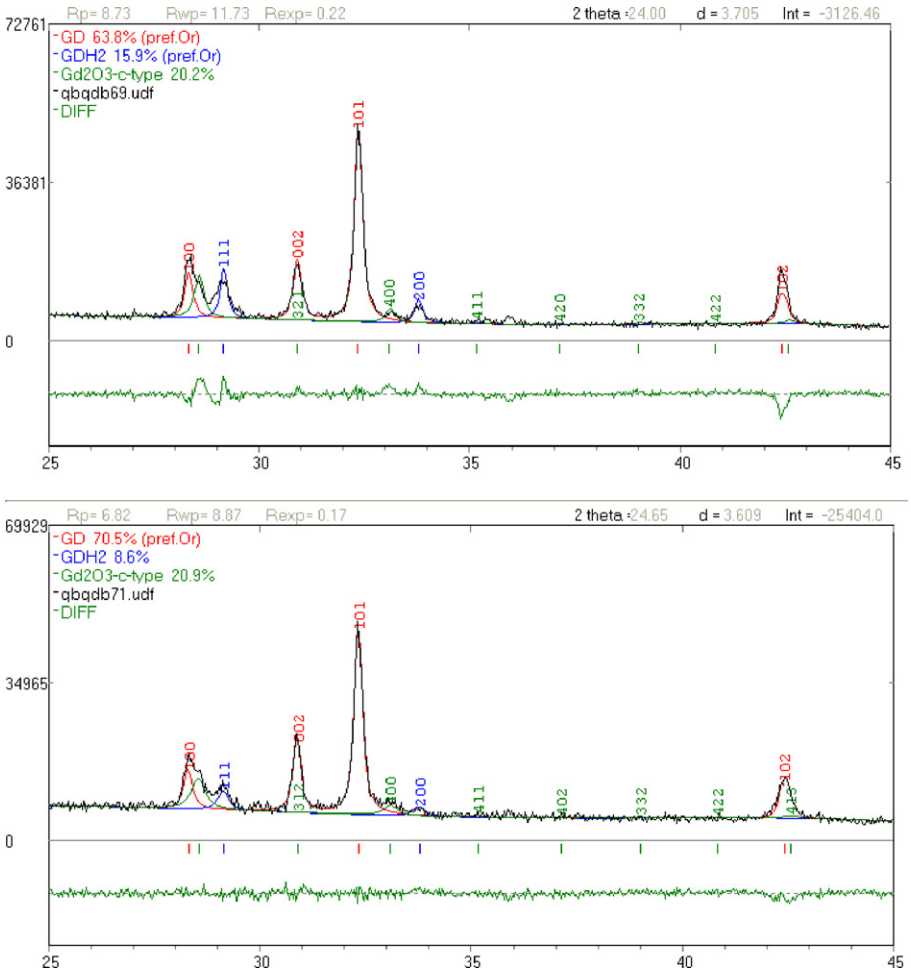

Fig. 3. *Continued*

from the Rietveld and LPF analyses and the GCs coverage estimated from the metallographic pictures. This correlation may substantiate the assignment of the $(1\,1\,1)_h$ orientation to the formation of the GCs.

4. Discussion

4.1. Orientation relations between the $(0\,0\,1)_h$ and $(1\,1\,1)_h$ planes of the cubic hydride and the $(0\,0.1)_m$ plane of the hexagonal metal

X-ray powder diffraction is not a tool for determination of orientation relations. However, it is reasonable to assume that the observed preferred planes of the cubic hydride (i.e., the $(0\,0\,1)_h$ plane at the lower temperature regime and the $(1\,1\,1)_h$ plane at the higher temperature range) form preferentially upon the hexagonal $(0\,0.1)_m$ habit plane of Gd (as in other hexagonal close-packed-HCP-metals). A preferred growth of the $(1\,1\,1)_h$ plane of FCC hydrides on the similar structure of the metal atoms – the hexagonal $(0\,0.1)_m$ plane of parent HCP metals – have been reported for similar metal-hydride systems (e.g. [5–8]). Hence, the fact that GdH_2 grows with M–H orientation relationship of $(0\,0.1)_m||(1\,1\,1)_h$ needs no further explanation. Nevertheless, the appearance of a single $(0\,0\,1)_h$ GdH_2 reflection in the low temperature range calls for supplementary discussion.

Before proceeding further, it is worthwhile to refer to the term "preferred orientation" in the context of polycrystalline systems. This term means that for some parent grains, the growth of the product nuclei takes place preferentially with a certain orientation relation relative to the parent plane. For some given parent grains having those preferred planes parallel to the surface, the XRD reflections related to the corresponding product orientation are preferentially counted compared to the random product growth mode.

Any hydride nucleus, forming initially as a single crystal on the parent metal grain, may grow to be polycrystalline due to the emergence of new nucleation points in the metal or when transpassing metal grain boundaries (especially for the larger GCs). The hydride phases should therefore be regarded as textured polycrystalline phases.

In the present case, the only hydride planes that were apparent in the XRD, were the $(0\,0\,1)_h$ at the lower temperature range, and a mixture of $(0\,0\,1)_h$ and the $(1\,1\,1)_h$ at the higher temperature range, indicating that other hydride growth modes had a relatively small contribution (below the detection limit of the XRD measurements). The $(0\,0\,1)_h$ line, arising from the "small family" hydride, results from the reflections of the whole population of small hydride nuclei. The width of the diffraction lines indicates that the upright size of the hydride is ~0.05–0.1 μm (consistent with the AFM result) while its width is 0.5–1 μm according to the AFM results.

In order to depict the structural relation between the $(0\,0\,1)_h$ plane of the GdH_2 FCC unit cell and the $(0\,0.1)_m$ plane of Gd, let us use an orthorhombic base central lattice as a presentation of the Gd unit cell. For such orthorhombic presentation, the hexagonal $(0\,0.1)_m$ basal plane of the HCP presentation is also assigned as the $(0\,0\,1)_m$ plane of the orthorhombic cell, but with the rectangular cell constants given by $a = 0.364$ nm, $b = a\sqrt{3} = 0.629$ nm and

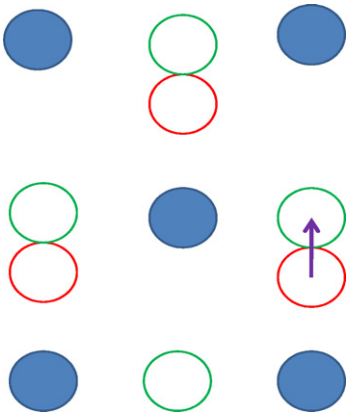

Fig. 4. Gd–HCP as orthorhombic base centered unit cell. Full spheres are for $z=0$; Other spheres are for $z=1/2$. Red and green spheres represent the position of Gd atoms in Gd and GdH_2 respectively. (For interpretation of the references to colour in Fig. 4 legend, the reader is referred to the web version of the article.)

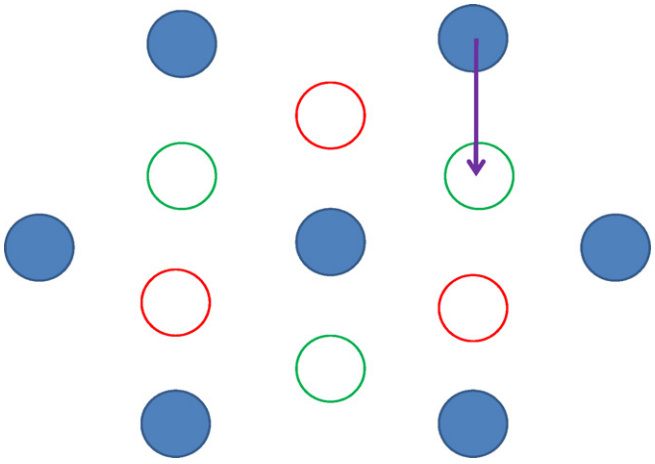

Fig. 5. Gd–HCP as hexagonal unit cell. Full spheres are Gd atoms for $z=0$; Red spheres are position of Gd atoms in Gd for $z=1/2$. Green spheres are position of Gd atoms in GdH_2 at $z=1$. (In Gd at $z=1$, the atoms are at the same positions as in $z=0$). (For interpretation of the references to colour in Fig. 5 legend, the reader is referred to the web version of the article.)

$c=0.5873$ nm. Fig. 4 illustrates this structure, and its relation to the $(0\,0\,1)_h$ plane of the hydride.

On the $(0\,0\,1)_m$ plane of the metal within this orthorhombic presentation (which actually corresponds to the $(0\,0.1)_m$ basal plane in the HCP presentation) the Gd atoms are stacked in two layers. Let us place the first layer of Gd atoms in the lattice points $(0,0,0)$ and $(1/2,1/2,0)$ (full blue) and the second one (open red) in positions $(0,1/3,1/2)$ and $(1/2,5/6,1/2)$, 0.2937 nm above the centroids of equilateral triangles of Gd atoms in the first layer. The average Gd–Gd interatomic distance in the Gd structure is $R_H=0.36$ nm. For the GdH_2 on the $(0\,0\,1)_h$ plane the Gd atoms are also stacked in two layers. The first layer of Gd in GdH_2 is similar to that in Gd $(0,0,0)$ and $(1/2,1/2,0)$ positions (full blue). However, the second layer is in $(0,1/2,1/2)$ and $(1/2,0,1/2)$ 0.29 nm above the first one (open green). The Gd–Gd inter atomic distance in the GdH_2 structure is $R_C=0.375$ nm. The shift in the atomic position between the Gd and the GdH_2 structures is only $R_H/(2\sqrt{3})$ in the Gd lattice. In order to complete the Gd to GdH_2 transition, where $(0\,0\,1)_m$ Gd parallel to $(0\,0\,1)_h$ GdH_2, all three cell parameters should become equal in Gd to those of GdH_2 (0.53 nm) by expansion along [1 0 0] direction and contraction along [0 1 0] and [0 0 1] directions in the orthorhombic Gd unit cell. Hence, a small shift of Gd atoms is required for the transformation to the hydride, with the orientation relations of $(0\,0.1)_m||(0\,0\,1)_h$ namely, $(0\,0\,1)_h$ hydride plane parallel to the basal plane of the hexagonal metal. This transformation involves anisotropic distortion of the corresponding metal lattice parameters, with a contraction in the [0 1 0], [0 0 1] direction, and an expansion in the [1 0 0] direction. In this case the ratio between the hydride and metal inteplanar distance normal to the surface is 0.92. Consequently, the growth of hydride along [0 0 1] direction normal to the surface does not apply a pressure on the oxide overlayer.

On the other hand, the growth of the $(1\,1\,1)_h$ hydride plane parallel to the hexagonal $(0\,0.1)_m$ metal plane, as depicted in Fig. 5, requires a larger shift of Gd atoms, and results in an almost isotropic expansion of the metallic unit cell, by about 5.2%. In this case the ratio between the hydride and metal inteplanar distance normal to the surface is 1.06. Consequently, the growth of hydride along [1 1 1] direction normal to the surface applies a pressure on the oxide overlayer.

4.2. Possible explanation of the texture change observed with increasing temperature

It has been observed that under some given hydriding conditions (hydrogen pressure of 6 mbar and exposure time of 480 s), increasing the reaction temperature above a certain value (473 K) causes a change in the texture characteristics of the precipitated hydrides (from a preferred $(0\,0\,1)_h$ orientation into a mixture of $(0\,0\,1)_h$ and $(1\,1\,1)_h$ with the latter orientation prevailing). Concurrent with this texture change, hydrides of the GCs "family" start to appear.

From other publications on similar structure M–H systems (an hexagonal parent metal converting into a cubic FCC hydride), it seems that the thermodynamic preference of precipitated hydride is to grow with its $(1\,1\,1)_h$ plane parallel to the $(0\,0.1)_m$ basal metal plane [5–8]. The question which may be addressed is: why at the lower temperature regime (below about 470 K), the preferred observed hydride growth plane is the $(0\,0\,1)_h$ and not the anticipated $(1\,1\,1)_h$ one?

There are two possible alternative explanations for the above observations. One explanation relates to the kinetic versus thermodynamic parameters that control the hydride precipitation. As discussed in Section 4.1, the growth of the $(1\,0\,0)_h$ parallel to the $(0\,0.1)_m$, requires a smaller displacement of Gd atoms than the corresponding growth of the $(1\,1\,1)_h$ plane (compare Fig. 4 to Fig. 5). Hence, even though the total misfit strain energy may be lower for the $(0\,0.1)_m||(1\,1\,1)_h$ growth, the activation energy for the $(0\,0.1)_m||(1\,0\,0)_h$ process may be lower. Consequently, at the lower temperature range, the kinetic parameters dominate over the thermodynamic ones, leading to the growth of the energetically less favorable, but the kinetically more favorable route. According to this view, the increase of temperature induces the change of hydride growth texture (by overcoming the kinetic barrier) which in turn causes the rupture of the oxidation overlayer and GCs formation.

Yet, if this was the case, we could anticipate that at temperatures above the initial temperature of the texture change (i.e., 470 K in our case), the preferred reflection from the GdH_2 $(1\,0\,0)_h$ plane would decrease with increasing temperature decaying totally well above the transition temperature. In that temperature range, the $(1\,1\,1)_h$ reflections would prevail the XRD patterns (since according to this view, also the small family spots should grow at that preferred orientation). This, however, is not obtained experimentally (as described in Section 3) and noticeable reflections of the $(1\,0\,0)_h$ planes still appear at the high temperature range, above the temperature of the texture change.

It is thus more likely that the different modes of preferred hydride growth are related to the different "families" of hydrides.

At the lower temperature range where only the small spots family forms, the compression of the overcoating oxidation layer prevents the development of the $(0\,0\,0.1)_m||(1\,1\,1)_h$ mode, due to the surface normal stress component that is associated with the isotropic expansion of this growth mode. In this regime, only the $(0\,0\,0.1)_m||(1\,0\,0)_h$ growth takes place, and is typical to the small spot family that develops under an intact oxidation overlayer. Increasing the temperature above a certain value enables the initiation of rupture at specific locations in the oxidation layer, which allows the development of the underlying hydride GCs, with the common preferred orientation. It is not clear why increasing the temperature induces cracking of the oxidation layer. This may be due to some mechanical changes induced in that layer (e.g. different thermal expansion coefficients of the oxide and the metal). An additional explanation, supported by the XRD results shown in Table 2, is that oxide crystallization occurs at the higher temperatures. This change in oxide structure leads to a less tough oxide layer, which breaks more easily than the thin, and probably amorphous, oxide layer that coats the metal before exposure (see Experimental section). In addition, oxide crystallization may induce oxide cracking at particular locations. In any case, the appearance of the preferred $(0\,0\,0.1)_m||(1\,1\,1)_h$ growth relation is apparently caused by the formation of the GCs (and not inversely like in the first view). And as long as the surface is composed of the two families, both texture patterns (i.e., the $(0\,0\,1)_h$ and the $(1\,1\,1)_h$) should be observed, as indeed obtained experimentally.

5. Conclusions

1. As reported in previous publications [1–4], exposing polycrystalline Gd samples to hydrogen, initiates hydride formation at the surface region by two sequential steps: (i) Rapid formation of small (sub-micrometric) hydride spots, which are formed beneath the thin oxidation overlayer that coats the surface. This "family" attains an almost constant size in the range of 0.5–1 μm, and practically ceases to grow. (ii) After a certain "induction time", some of the formed hydride spots (GCs) break the oxidation layer and start to grow at constant velocity. The induction time for the initiation of stage is dependent on the specific hydriding conditions, decreasing with the increase of both pressure and temperature.
2. A preferred orientation of the hydride $(0\,0\,1)_h$ plane develops for the "small family" precipitation and converts to a preferred $(1\,1\,1)_h$ plane for the GCs development.
3. Assuming both hydride planes grow parallel to the $(0\,0\,0.1)_m$ metal hexagonal basal plane, a different expansion isotropy characterizes the two above texture modes. For the $(0\,0\,0.1)_m||(1\,0\,0)_h$, a contraction occurs along the surface normal direction (and expansion in one of the surface parallel directions), whereas for the $(0\,0\,0.1)_m||(1\,1\,1)_h$, an almost isotropic expansion occurs for all directions.
4. The stress component that is exerted by the oxidation overlayer on the developing hydride (normal to the surface) thus seems to prevent the $(0\,0\,0.1)_m||(1\,1\,1)_h$ growth mode, leading to the $(0\,0\,0.1)_m||(1\,0\,0)_h$ preferred orientation. This stress component vanishes as the oxidation layer is ruptured, leading to the energetically favored growth of the $(0\,0\,0.1)_m||(1\,1\,1)_h$, for the GCs.

Acknowledgements

This work was partially supported by a grant from the Israel Council for Higher Education and Israel Atomic Energy Commission and a grant from the Ministry of National Infrastructure, Division of R&D.

The authors would like to thank S. Cohen and A. Schwartz for the AES measurement, G. Rafailov for the X-Ray measurement, N. Samir for many helpful discussions and to T. Even-Hen, Y. Alfi and S. levi, for their technical support.

References

[1] M.H. Mintz, in: K.H.J. Buschow, R.W. Cohn, M.C. Flemings, B. Ilschner, K.J. Kramer, S. Mahajan (Eds.), Encyclopedia of Materials: Science and Technology, Elsevier Sci., 2002, pp. 1–9.
[2] Y. Ben-Eliyahu, M. Brill, M.H. Mintz, J. Chem. Phys. 111 (1999) 6053.
[3] R. Arkush, A. Venkert, M. Aizenshtein, S. Zalkind, D. Moreno, M.B. rill, M.H.M. Mintz, N. Shamir, J. Alloys Compd. 244 (1996) 197.
[4] G. Benamar, D. Schweke, J. Bloch, T. Livneh, M.H. Mintz, J. Alloys Compd. 477 (2009) 188.
[5] Y. Greenbaum, D. Barlam, M.H. Mintz, R.Z. Shneck, J. Alloys Compd. 509 (2011) 4025.
[6] J.F. Bingert, R.J. Hanrahan Jr., R.D. Field, P.O. Dickerson, J. Alloys Compd. 365 (2004) 138.
[7] T.B. Scott, G.C. Allen, I. Findlay, J. Glascott, Philos. Mag. 87 (2006) 177.
[8] D. Moreno, R. Arkush, S. Zalkind, N. Shamir, J. Nucl. Mater. 230 (1996) 181–186.
[9] A. Danon, J.E. Koresh, M.H. Mintz, Langmuir 15 (1999) 5913.
[10] D.F. Teter, R.J. Hanarhan,C. J/Wetteland, Los Alamos National Laboratory Report, LA-13772-MS, March, 2001.
[11] Y. Greenbaum, D. Barlam, M.H. Mintz, R.Z. Shneck, J. Alloys Compd. 452 (2008) 325.
[12] V.S. Arunachalam, B. Lehtinen, G. Ostberg, J. Nucl. Mater. 21 (1967) 241.
[13] K. Une, S. Ishimoto, J. Nucl. Mater. 357 (2006) 147.
[14] K. Une, S. Ishimoto, J. Nucl. Mater. 389 (2009) 436.
[15] N.A.P. Kiran Kumar, J.A. Szpunar, Z. He, J. Nucl. Mater. 403 (2010) 101.
[16] J. Bloch, M.H. Mintz, J. Less-Common Met. 166 (1990) 241.
[17] G. Benamar, D. Schweke, N. Shamir, S. Zalkind, T. Livneh, A. Danon, G. Kimmel, M.H. Mintz, J. Alloys Compnd. 498 (2010) 26.
[18] H.M. Rietveld, J. Acta Cryst. 22 (1967) 151.
[19] H.M. Rietveld, J. Appl. Cryst. 2 (1969) 65.
[20] D.B. Wiles, R.A. Young, J. Appl. Cryst. 14 (1981) 149.
[21] K. Kraus, G. Nolze, J. Appl. Cryst. 29 (1996) 301.